Design & Analysis of a Hot Air-Assisted Flying Wing UAV with Solar Energy Systems for Flight Time Enhancement

Design & Analysis of a Hot Air-Assisted Flying Wing UAV with Solar Energy Systems for Flight Time Enhancement

Abdelrahman A. Shahin[1], Ezzeldeen M. Aboelkasim[1], Abdelrahman E. Awad[1], Ali A. Sakr[1], Amr K. Balat[1], Mahmoud A. Hassanein[2], Sara A. El-Bahloul[2,3*], Wael Seddik Moustafa[2,4]

[1] Aeronautical & Aerospace Engineering Program, Faculty of Engineering, New Mansoura University, New Mansoura, Egypt
[2] Faculty of Engineering, New Mansoura University, New Mansoura, Egypt
[3] Production & Mechanical Design Engineering Department, Faculty of Engineering, Mansoura University, Mansoura, Egypt
[4] Architectural Engineering Department, Faculty of Engineering, Mansoura University, Mansoura, Egypt
*E-mail: sara.elbahloul@nmu.edu.eg

Abstract. The growing demand for energy-efficient unmanned aerial vehicles (UAVs) has spurred research into alternative power and lift-enhancing mechanisms to improve flight duration and operational efficiency. Solar film technology has been widely explored, offering lightweight energy solutions that significantly extend UAV endurance. However, integrating active hot air lift mechanisms with solar energy systems remains largely unexplored. This research bridges this gap by proposing and analyzing a hybrid UAV system that incorporates solar film technology and onboard hot air lift-enhancing mechanisms. The proposed system aims to optimize energy utilization and increase flight duration by leveraging the complementary properties of solar and thermal technologies. Using a design of experiments (DOE) approach, the optimal configuration was identified as an ogival delta wing shape, S1223 airfoil, and 150°C hot air system. Results showed a 3.86% reduction in apparent weight due to hot air buoyancy, enhancing flight endurance by approximately 4% compared to a solar-only configuration. These findings demonstrate the viability of integrating solar and thermal systems for energy-efficient and sustainable UAV design.

Keywords: Hot Air-Assisted UAV; Flying Wing UAV; Solar Energy Systems; Flight Time Enhancement; Energy Efficiency; Solar-Heated UAV; Sustainable UAV Design

1. Introduction

Unmanned aerial vehicles (UAVs) have emerged as critical tools in various industries, including environmental monitoring, military operations, and disaster management, owing to their adaptability and efficiency. However, one of the primary challenges in UAV operations is optimizing flight endurance while maintaining energy efficiency. Research into renewable energy systems, such as solar film technology, has shown promising results in extending UAV flight

duration by leveraging lightweight and flexible photovoltaic materials [1], [2]. These advancements have significantly improved energy-to-weight ratios, enabling UAVs to sustain longer missions without compromising structural integrity [1], [3].

Despite these advancements, the potential of integrating active hot air lift mechanisms with solar energy systems remains unexplored. Current research focuses predominantly on passive thermal systems, such as natural updrafts, or single-source power solutions, such as solar energy or batteries [4], [5]. This creates a significant gap in the development of hybrid UAV systems that combine solar power and onboard thermal lift mechanisms to optimize energy use and enhance flight capabilities [1], [5].

The purpose of this study is to address this gap by designing, developing, and analysing a hybrid UAV system that integrates solar film technology with active hot air lift mechanisms. By combining these technologies, the proposed system aims to achieve superior energy efficiency and flight endurance compared to conventional solar-powered UAVs. This research contributes to the growing field of sustainable aviation, providing an innovative solution to enhance UAV performance in energy-constrained environments.

2. Literature Review

2.1 Solar Film Technology in UAVs

Solar film technology has been widely explored as a means to enhance UAV flight duration and energy efficiency. Lightweight and flexible photovoltaic cells, such as copper indium gallium selenide (CIGS) and multi-junction solar cells, have demonstrated significant improvements in energy-to-weight ratios, enabling longer missions with minimal structural impact [1], [2]. Studies have also highlighted the benefits of advanced energy management systems, such as Maximum Power Point Tracking (MPPT), which optimize energy harvesting under varying solar conditions [3]. These advancements have made solar-powered UAVs a viable option for applications requiring extended endurance, such as surveillance and disaster relief [1], [3].

2.2 Thermal Lift Mechanisms

While solar technologies are well-documented, research on leveraging thermal lift mechanisms remains limited. Existing studies briefly mention the use of natural thermals, such as updrafts, to augment UAV flight efficiency. However, these approaches are passive and depend heavily on environmental conditions, which restrict their applicability [4], [5]. No research to date has explored the integration of active onboard hot air systems to enhance lift capabilities, highlighting a critical gap in the literature [4].

2.3 Hybrid UAV Systems

Hybrid UAV systems, which combine multiple energy sources or lift mechanisms, represent a promising avenue for improving flight performance. Some studies have explored combining solar and battery systems, achieving notable gains in endurance through modular designs and energy optimization strategies [5]. However, the integration of solar energy with active thermal lift mechanisms remains unexplored, presenting an opportunity to develop UAVs that can autonomously optimize energy usage and lift during flight [1], [5]. This research aims to bridge this gap by proposing a novel hybrid system that leverages the complementary benefits of solar film technology and hot air lift-enhancing mechanisms.

3. Methodology

3.1 Design Framework

The design of the hybrid UAV system integrates solar film technology and hot air lift-enhancing mechanisms to optimize flight duration and energy efficiency. The UAV structure was modelled using lightweight composite materials to minimize overall weight while maintaining structural integrity. Flexible solar films, such as CIGS photovoltaic cells, were selected for their high energy-to-weight ratio and ease of integration into the UAV's aerodynamic design [1], [5]. The onboard hot air lift mechanism was designed to generate additional lift by heating the air within a controlled chamber, reducing reliance on propulsive thrust for sustained flight [4].

Design of Experiments method is selected by performing a factorial design to get to the optimal configuration [6]. Considering the factors and levels shown in Table 1 to enhance flight

Table 1. Factors and levels table used in the design of experiments performed.

Factor	Level 1	Level 2	Level 3
Airfoil	S1223	Eppler 387	Clark Y
Wing Shape	Delta	Ogival Delta	Swept
Propulsion System	Brushed DC Motor	BLDC Motor	Hybrid Propulsion
Air Temperature (^{o}C)	100	120	150

time by consuming less power and relying on the lift force generated from the hot air balloon to give the body the buoyancy required to maintain airborne without consuming lots of energy [7].

Performing a full factorial design, making the constraints to generate higher lift, maximize flight time and minimizing air density and power consumption [6],[8]. The considered response variables is the lift coefficient (c_L) for the airfoil factor, span efficiency (e) for wing shape factor, and thrust for the propulsion system and density for air temperature [6], [7],[21],[22].

Based on the previous considerations and the full factorial design performed, the results are

Table 2. Comparison of the considered airfoil characteristics [16],[17],[18].

Airfoil	(C_L)	(C_D)	Lift-to-Drag Ratio (L/D)
S1223	1.2	0.03	40
Eppler 387	1.1	0.04	27.5
Clark Y	1.0	0.05	20

concluded in Table 3. Figure 1 illustrates the optimizer tool that was used during the DOE with the help of MINTAB Software.

Table 3. Comparison of the considered airfoil characteristics [16],[17],[18].

Factor	Optimal Level
Airfoil	S1223
Wing Shape	Ogival Delta (e = 0.92)
Propulsion System	Hybrid Propulsion
Air Temperature	150 °C

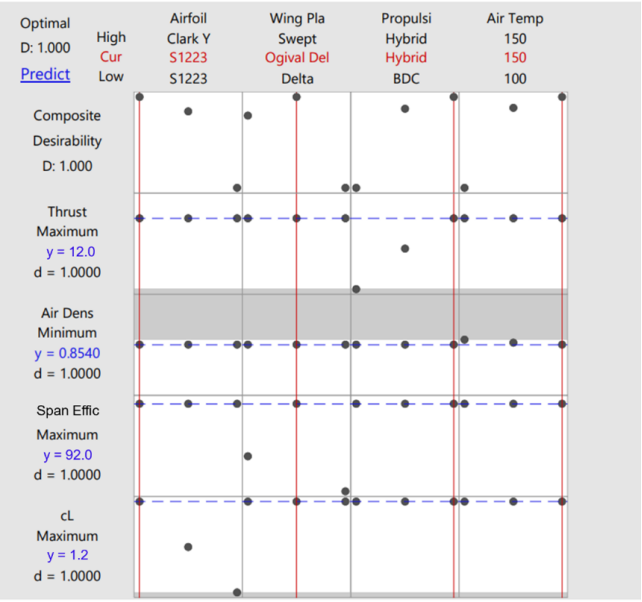

Figure 1. Optimization plot resulted from the full factorial DOE performed including airfoil selection, wing planform, propulsion type, and air temperature. The composite desirability score (1.000) indicates optimal performance for maximum thrust (12.0), minimum air density (0.8540), maximum span efficiency (92%), and maximum lift coefficient (1.2). Key configurations include the S1223 airfoil, ogival delta wing planform, and hybrid propulsion system at air temperature of 150°C.

3.2 Energy System Modelling

An energy model was developed to simulate the hybrid UAV's power flow during flight. The model incorporates energy harvested from solar films, power consumed by propulsion and electronics, and thermal energy used for lift generation. The Maximum Power Point Tracking (MPPT) algorithm was implemented to optimize solar energy utilization under varying sunlight conditions [3].

3.2.1. Lifting Force Analysis with Solar Heaters

The lifting force for the hot air-assisted UAV is generated using solar heaters, which raise the temperature of the air within the balloon. The buoyant force, F_b, responsible for offsetting part of the UAV's weight, is expressed in Equation (1). [9], [10]

$$F_b = g \cdot V \cdot (\rho_{ambient} - \rho_{hot\ air}) \quad (1)$$

where:

- V: Volume of the hot air balloon.
- $\rho_{ambient}$: Density of ambient air (1.225 kg/m^3 at standard sea level and temperature).
- $\rho_{hot\ air}$: Density of hot air, calculated using the ideal gas law illustrated in Equation (2). [9], [10]

$$\rho_{hot\ air} = P/(R \cdot T_{hot\ air}) \quad (2)$$

where:

- P: Atmospheric pressure (101.3 kPa).
- R: Specific gas constant for air (287 J/(kg·K)).
- $T_{hot\ air}$: Absolute temperature of the hot air (in Kelvin).

The solar heaters provide the thermal energy to heat the air, with the heating power Q heat defined as in Equation (3). [9], [10]

$$Q_{heat} = \eta_{heater} \cdot A_{heater} \cdot I \quad (3)$$

where:

- η_{heater}: Efficiency of the solar heater system.
- A_{heater}: Effective surface area of the solar heaters.
- I: Solar irradiance (800 - 1000 W/m^2 in direct sunlight).

The percentage of lift force generated by the hot air relative to the UAV's total weight is Calculated using Equation (4). [11]

$$Percentage\ Contribution = \frac{F_{Lift}}{W_{UAV}} \times 100 \quad (4)$$

The size and configuration of the balloon are optimized to balance the required lift, material weight, and structural stability. This solar heating mechanism eliminates the need for fuel-based burners, reducing system weight and improving sustainability. Lightweight, thermally resistant balloon materials, such as aluminized polyester, are employed to retain heat efficiently [11].

3.2.2. Flight Time Enhancement with Dual Systems

The endurance of the UAV is enhanced by reducing its effective weight through hot air buoyancy and supplying power to its electric systems using film solar panels. The total flight time, $T_{hot\ air}$, is modelled as in Equation (5). [12], [13]

$$T_{hot\ air} = T_{original} \cdot (m_{original} / m_{effective}) \quad (5)$$

where:

- $m_{effective} = m_{original} - F_b / g + m_{system}$.
- F_b: Buoyant force generated by the hot air system.
- m_{system}: Weight of the hot air balloon, solar heaters, and panels.

The film solar panels generate electrical power to drive the UAV's propulsion and control systems is calculated using Equation (6). [12], [13]

$$P_{solar} = \eta_{panel} \cdot A_{panel} \cdot I \quad (6)$$

where:

- η_{panel}: Efficiency of the solar panels.
- A_{panel}: Surface area of the panels.
- I: Solar irradiance.

3.3 Aerodynamic and Thermal Analysis

The aerodynamic performance of the hybrid UAV was analysed using computational fluid dynamics (CFD) simulations. Key parameters, such as lift-to-drag ratio and stability margins, were evaluated to determine the impact of solar film placement and hot air lift mechanisms on overall flight efficiency [2], [5]. Thermal simulations were conducted to optimize the heat distribution within the onboard lift system, ensuring uniform airflow and minimizing energy losses.

The design of the hot air-assisted UAV was carried out using SOLIDWORKS, leveraging its advanced parametric modeling and simulation tools to create a streamlined and efficient configuration. The flying wing design with an ogival delta shape was chosen for its aerodynamic efficiency and compatibility with the integrated systems.

4. CAD Model & System Design Features

4.1 CAD Model: Dimensions and Material

The hot air-assisted UAV's dimensions, featuring a 0.8 m root chord and a 0.06 m tip chord, 1.21 m wingspan, and 0.59 m maximum height, are optimized for aerodynamic efficiency, structural integrity, and thermal system integration. The S1223 airfoil ensures high lift-to-drag performance in low speeds, while the ogival delta shape enhances stability. The volume of the hot air bag inside the UAV can reach up to 75 Liters which was one of our main design considerations to increase the hollow volume inside the UAV as much as possible to embed the hot air balloon and have sufficent static lift. The 0.59 m height supports structural reinforcements and accommodates internal components, such as hot air ducts and solar wiring. These compact dimensions also enable portability and efficient integration of dual power systems, meeting the UAV's design objectives for extended flight times and operational versatility.

The selected material for the UAV's body is lightweight polyurethane for its durability and resistance to environmental factors, with an Aerokote coating to enhance aerodynamics and protection. This design ensures a robust, efficient structure, with the total mass of the UAV kept

(a) (b) (c)

Figure 2. CAD model of the UAV: (a) isometric view; (b) sectional view, and (c) bottom view

at 700 grams to optimize flight performance. Figure 2 illustrates the CAD model of the UAV.

The analysis of the hot air-assisted UAV encompasses aerodynamic, thermal, and electrical performance evaluations to validate the overall design. Aerodynamic analysis determines lift and drag forces in addition to analytical lift distribution, thermal analysis examines heat distribution

and insulation efficiency, and electrical analysis evaluates the integration of solar panels and power management systems. These simulations provide a comprehensive understanding of the UAV's performance under operational conditions, ensuring its functionality and efficiency.

4.2 System Design Features

4.2.1. Propulsion Systems:

The propulsion system for the UAV, with an original weight of 700 grams, was designed to meet both VTOL and forward flight requirements. To account for uncertainties and provide a safety factor, calculations were performed with a total weight of 1 kg. For VTOL, the thrust requirement was calculated using a thrust-to-weight ratio (T/W) of 1.2, and will equal to about 1200 $g\ thrust$

A 64mm EDF was selected for VTOL, providing 1200 g thrust at 450 W power consumption on a 4S LiPo battery.

For rear propulsion, the thrust required to overcome drag was calculated using the drag equation (7). The thrust is equals to about 35 g thrust. With a safety factor of 2 applied to account for climb and manoeuvring the T_{Rear} will equals to about 70 g thrust

$$T_{Cruise} = \frac{1}{2}\rho v^2 C_D A \tag{7}$$

A 40mm EDF was chosen for rear propulsion, delivering 200 g thrust at 60 W power consumption, as supported by performance testing of small-scale propulsion systems [19]. Battery endurance was calculated using a 4S LiPo battery (14.8 V, 3 Ah, 44.4 W):

$$T_{VTOL} = \frac{44.4\,W}{450\,W} \times 60 = 5.92\,minutes, \qquad T_{Cruise} = \frac{44.4\,W}{60\,W} \times 60 = 44.4\,minutes.$$

The design ensures sufficient thrust for VTOL and efficient forward flight, with sufficient endurance for mission requirements [20].

4.2.2. Hot Air Balloon and Solar Systems:

The black regions visible in the design represents the film solar panels and solar heaters and its area is about 0.14 m^2. The solar panels generate electrical power, while the heaters contribute to thermal energy for the hot air system, enhancing flight time and altitude control. While the hot air balloon is embedded inside the UAV's body and along all axis. The analysis of this system will be demonstrated further in the upcoming sections.

4.2.3. Aerodynamic Design:

As mentioned before the S1223 airfoil was selected due to its characteristics and its classification as a low Reynolds number airfoil which contributes in generating lift at very low speed causing the rear thruster to operate at low energy resulting in energy saving. An ogival delta planform was considered for its high span efficiency which is near elliptical causing the structure of the design more stable. The big height of the UAV which is clearly illustrated in Figure 2 was made to ensure that the interior volume is sufficient to contain the hot air balloons and to generate static lift taking into account that the aerodynamic forces are not affected negatively in a big percentage.

5. Aerodynamics and Thermal Analysis

5.1 Aerodynamics Analysis

The aerodynamic analysis of the UAV's flying wing configuration was conducted using SolidWorks Flow Simulation to evaluate its lift and drag characteristics. The analysis involved determining lift and drag forces at varying velocities to assess the wing's aerodynamic efficiency. Simulation results provided quantitative insights into these forces, enabling an evaluation of the wing's performance and optimization for prolonged flight. This analysis is crucial in ensuring the design achieves an optimal balance between thrust, lift, and drag forces.

Figure 3 illustrates the flow simulation setup and reference axis, setting global goals as Force (Y) for (Lift) and Friction Force (Z) for (Drag). Five simulation runs were performed under consistent mesh settings and defined goals. The analysis began at a velocity of 5 m/s, with the speed incrementally increased by 5 m/s for each subsequent run, culminating at 25 m/s.

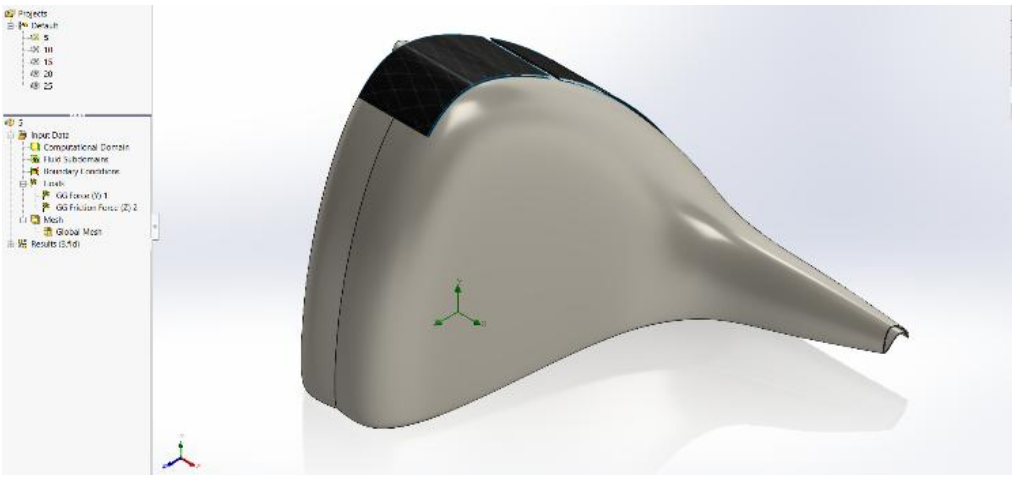

Figure 3. Flow simulation setup and reference axis.

5.2 Thermal Analysis

A comprehensive thermal analysis was performed in SolidWorks Flow Simulation to assess the UAV's aerodynamic performance under thermal conditions. The study focused on simulating internal fluid flow, with air chosen as the working fluid. The fluid subdomain was defined as the UAV's interior to replicate the thermal environment within the structure. Boundary conditions were applied, setting the wall temperature to a constant 30°C, while the interior air temperature was specified as 150°C at atmospheric pressure to simulate hot air-assisted propulsion scenarios. The global simulation goal was defined as the force in the Y-axis, representing the lift generated by the hot air in the UAV. This methodology allowed for an integrated analysis of thermal and aerodynamic interactions, providing valuable insights into the influence of internal heat flow on the UAV's lift performance and overall design optimization.

6. Results and Discussion

6.1 Theoretical Results

6.1.1. Analysis of Lift Contribution from Hot Air at 150 °C

A 75-liter hot air chamber at 150 °C was analysed for its contribution to the UAV's lift force. Using Equation (1) and substituting by the values: $V = 0.075\ m2$, $g = 9.81\ m/s^2$, $\rho_{ambient} = 1.2\ kg/m^3$, and $\rho_{hot\ air} = 0.84\ kg/m^3$, then the F_{Lift} will equals to 0.2649 N

The UAV has a total weight (W_{UAV}) of 700 g = 6.867 N. The percentage of lift force generated by the hot air relative to the UAV's total weight is Calculated using Equation (4) and is equal to 3.86 %

These results show that the lift generated by 75 liters of hot air at 150°C contributes approximately 3.86% of the total weight, effectively reducing the apparent weight of the UAV by this percentage. This reduction in weight could help decrease the load on the propulsion system, improving energy efficiency and potentially extending the flight duration.

6.1.2. Heating Analysis of 75 Liters of Air Using Solar Heaters:

Equation 3 is used to calculate the thermal energy provided by the solar heater taking into account $\eta_{heater} = 0.236$ [23], $A_{heater} = 0.14\ m^2$ (estimated from CAD model), and I: Solar irradiance (800 - 1000 W/m^2 in direct sunlight), the heating power ranges from: $Q_{heat} = 26.43 – 33.04\ W.$

To evaluate its sufficiency, the energy required to heat 75 Liters (0.075 m3) of air from 25 ^{o}C to 150 ^{o}C is calculated. Using the ideal gas law, the air mass is equal to 0.089 kg. The energy required to heat 75 Liters (0.075 m^3) of air from 25°C to 150°C is calculated using Equation (8).

$$Q_{Required} = m_{Air} \cdot c_p \cdot \Delta T \tag{8}$$

where m_{Air}=0.089 kg, c_p=1005 J/(kg·K) is the specific heat capacity of air, and ΔT=125 K is the temperature change. The required energy is 11,178.75 J (3.11 W). With the solar heater system providing 26.43–33.04 W. Using Equation (9), the air can be heated in approximately 5.63–7.05 minutes, demonstrating the system's sufficiency for this application. For faster heating or continuous operation, increasing the surface area may be necessary.

$$t = \frac{Q_{Required}}{Q_{Heat}} \tag{9}$$

6.1.3. Flight Time Improvement

The endurance of the hot air-assisted UAV was analyzed using the effective mass model, considering the total system mass of 700 grams, which includes the UAV body, hot air balloon, heaters, and all integrated components. The buoyant force generated by the hot air system, calculated as F_b=0.2649 N, offsets approximately 3.86% of the UAV's total weight, reducing the effective mass during flight to 0.673 kg.

Substituting in Equation (5), the new flight times for both VTOL and cruise phases were recalculated based on the data presented in subsection 4.2.1, which concluded the UAV's initial flight durations as 5.92 minutes for VTOL and 44.4 minutes for cruise. Applying the effective mass correction, the flight times were extended to about 6.16 minutes for VTOL Flight, and 46.18 minutes for Cruise Flight, with setting the original mass to be 1 kg for safety considerations.

This enhancement demonstrates the effectiveness of integrating the hot air buoyancy system, as it leads to an increase in total flight endurance without additional energy consumption. The

results further validate the hybrid UAV system's potential for extended flight missions by leveraging both solar energy and thermal lift mechanisms.

In Figure 4, UAV endurance as a function of solar irradiance, cruise speed, and battery capacity. Higher solar irradiance and battery capacity enhance endurance, emphasizing efficient solar panel use and lightweight, high-capacity batteries. Cruise speed presents a trade-off, where excessive speeds reduce endurance, highlighting the need for optimal velocity. Optimizing these factors can significantly improve flight efficiency and duration. Thus, improving the design is achievable when optimizing each factor.

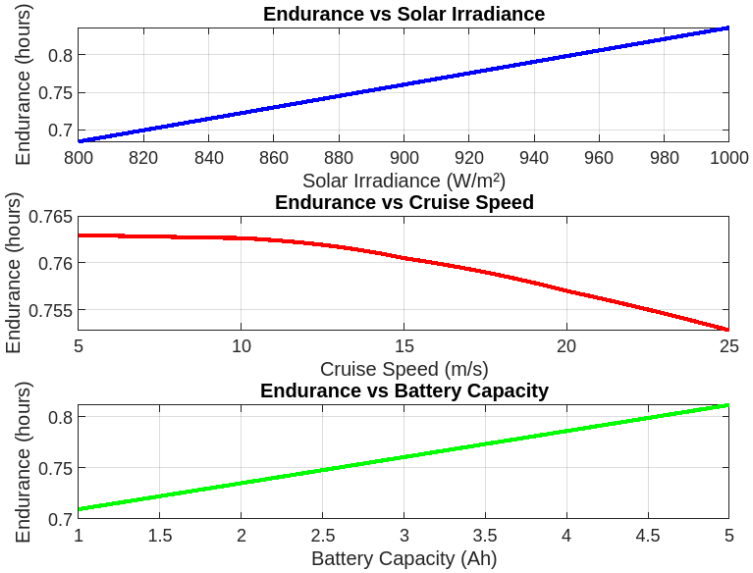

Figure 4. A graph illustrating the relation between endurance and various factors.

6.2 Analysis Results

6.2.1. Aerodynamics Analysis Results

Figure 5 illustrates the variation of lift and drag forces with velocity as obtained from the flow simulation results illustrated in Table 4. The lift force increases non-linearly with velocity, consistent with theoretical expectations, as lift is proportional to the square of velocity in subsonic flow regimes. Notably, at a velocity of 15 m/s, the UAV generates a lift force of 10.3 N, which is sufficient to lift the 700-gram UAV (equivalent to approximately 6.87 N of weight). This demonstrates that the UAV achieves optimal lift performance at this velocity, ensuring reliable flight capability.

Table 4. Flow simulation results at variable velocities.

Velocity (m/s)	Lift Force (N)	Drag Force (N)	C_L
S1223	1.2	0.03	40
Eppler 387	1.1	0.04	27.5
Clark Y	1.0	0.05	20

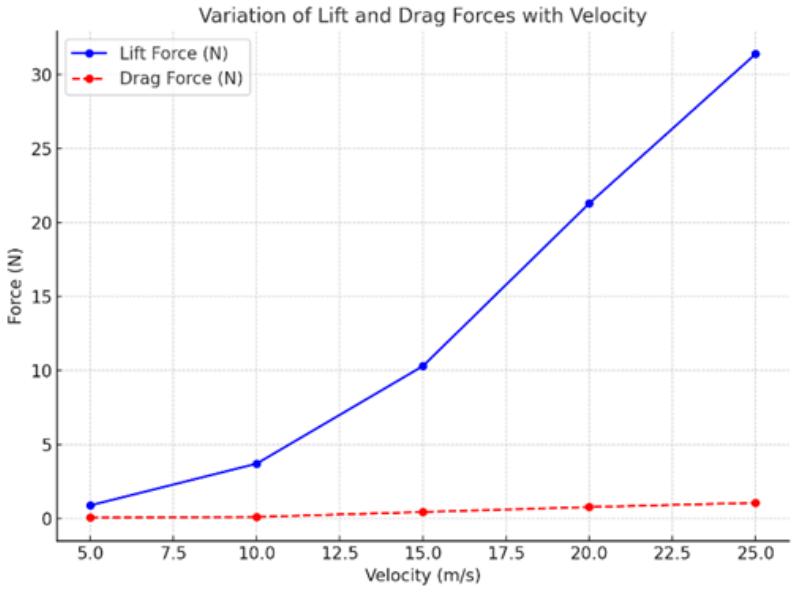

Figure 5. A graph illustrating variation of lift and drag forces with velocity

Conversely, the drag force increases with velocity but remains relatively small compared to the lift force. This indicates that the UAV's aerodynamic design effectively minimizes drag, enhancing its energy efficiency and flight endurance. The findings highlight the UAV's capability to produce substantial lift with minimal drag, supporting its suitability for hot air-assisted propulsion and extended flight applications.

Furthermore, lift distribution analysis was performed using MATLAB software to assess the lift over the span of the UAV. The governing Equation (10) used in this analysis is used to calculate the lift distribution over elliptical planforms, and it was used for this UAV design due to the similarity between the characteristics of the ogival delta and elliptical planforms [21].

$$L'(y) = L'_{max}\sqrt{1-\left(\frac{2y}{b}\right)^2} \tag{10}$$

where $L'_{\max} = \frac{4L}{\pi b}$ = 10.84 N, L = 10.3 N (from Table 4 at 15 m/s), b= 1.21is the wing span, and y is the location along span. Figure 6 illustrates the analysis results of the lift distribution along the wing span.

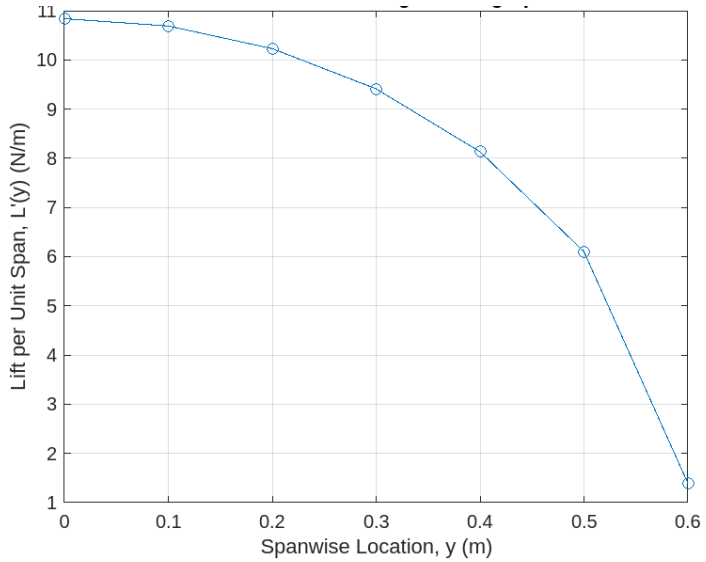

Figure 6. Lift distribution analysis results

6.2.2. Stability Analysis

The longitudinal stability analysis performed on MATLAB software reveals that the system exhibits 100% stability across all tested velocities, as indicated by the eigenvalues having negative real parts. The resulted static margin of 0.250 confirms positive longitudinal stability, which is essential for stable flight. At increasing velocities (5.0 m/s to 25.0 m/s), the eigenvalues demonstrate a consistent trend: the real parts become more negative (e.g., -4.603 at 5.0 m/s to -23.017 at 25.0 m/s), while the imaginary parts increase slightly (e.g., ±0.468i at 5.0 m/s to ±2.342i at 25.0 m/s). This indicates that the system becomes more damped and stable at higher velocities, with oscillatory behavior characterized by the imaginary components. These results confirm robust stability across the operational range. Figure 7 illustrates the longitudinal stability analysis results

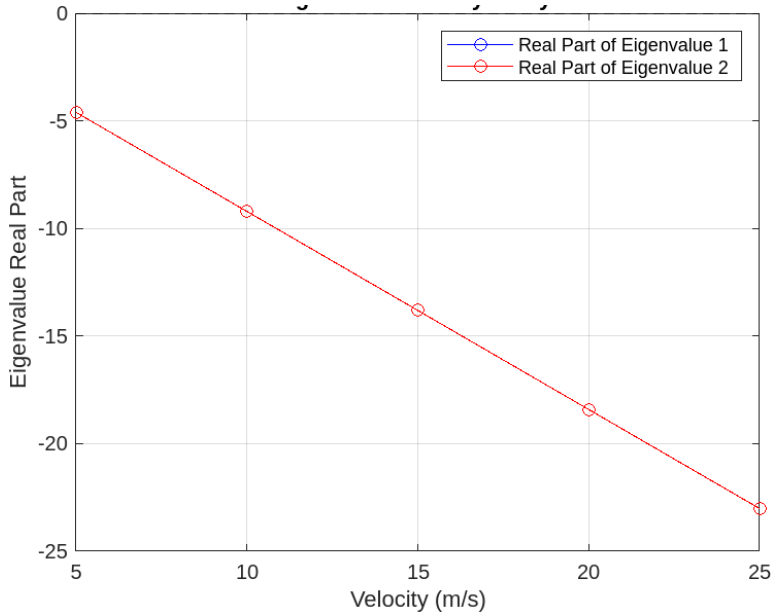

Figure 7. A graph illustrating stability analysis results

6.2.3. Thermal Analysis Results

As shown in Figure 8, the internal temperature distribution within the UAV was analyzed, with air at 150°C and wall temperature set to 30°C. The simulation revealed a lift force of 0.34 N, highlighting the impact of internal thermal conditions on the UAV's aerodynamic performance.

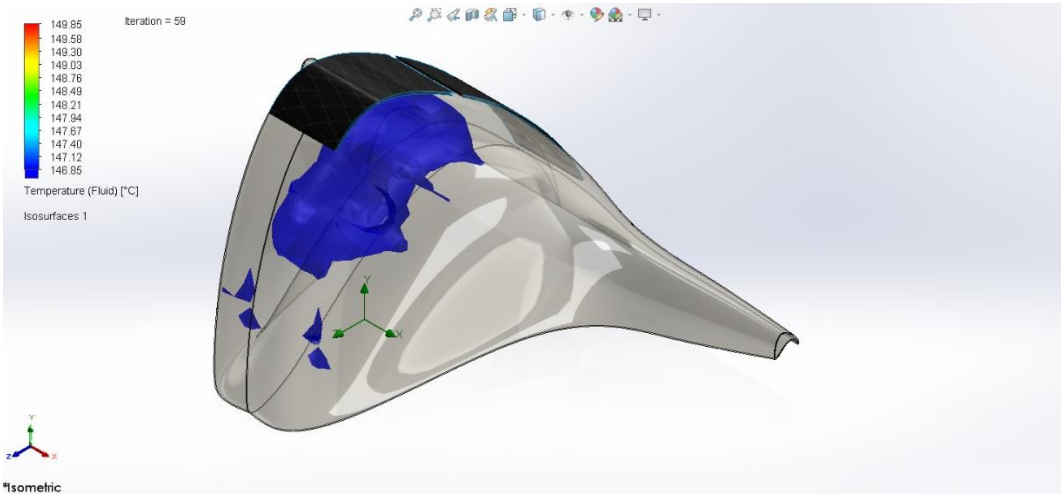

Figure 8. Thermal analysis results visualizing the hot air flow and temperature inside the UAV.

7. Conclusion

This study successfully developed and analyzed a hybrid flying wing UAV system incorporating solar energy systems and onboard hot air lift mechanisms. The integration of these systems resulted in significant enhancements in energy efficiency and flight duration. The DOE method identified an optimal configuration featuring an ogival delta wing shape, S1223 airfoil, and a 150°C hot air system, achieving a 3.86% apparent weight reduction and a 4% improvement in flight endurance. The aerodynamic, thermal, and energy analyses validated the feasibility of this novel design, demonstrating its potential to address the growing need for sustainable and efficient UAV technologies.

The results underline the benefits of combining solar and thermal systems for UAV applications, particularly in scenarios requiring prolonged missions and energy conservation. By reducing reliance on conventional propulsion systems, the proposed hybrid design sets a new benchmark for renewable energy integration in UAVs.

The proposed UAV design combines solar energy and hot air lift to enhance flight endurance but faces challenges in thermal management, weight, energy efficiency, aerodynamics, and system complexity. Addressing these issues through advanced materials, optimized integration, and extensive testing is essential for feasibility and practical application.

Future work will explore using lighter gases like helium, heated helium, or hydrogen to improve buoyancy. It will also focus on advanced materials, optimizing energy systems, and validating the design through dynamic testing. Application-specific adaptations for missions such as surveillance and disaster relief will also be pursued.

References

[1] R. K. Phanden, J. Chhabra, and B. S. Sikarwar, "An experimental study on the flight time of quadcopter using solar energy," Materials Today: Proceedings, vol. 26, pp. 210–215, 2020. [Online]. Available: https://doi.org/10.1016/j.matpr.2020.07.199.

[2] G. de Carvalho Bertoli, G. J. Adabo, et al., "Extending flight endurance of electric unmanned aerial vehicles through photovoltaic system integration," in Proc. Renewable Energy Research and Applications Conference, 2015, pp. 540–547.

[3] Liu, "Energy-optimal flight of a solar-assisted unmanned aerial vehicle," International Journal of Energy Optimization and Engineering, vol. 12, no. 2, pp. 1–15, 2022.

[4] P. Edi, N. Yusoff, and A. A. Yazid, "The design improvement of airfoil for flying wing UAV," WSEAS Transactions on Applied and Theoretical Mechanics, vol. 3, no. 9, pp. 809–819, 2008. [Online]. Available: https://www.researchgate.net/publication/236657704.

[5] Z. Lai, "Optimization of endurance performance for quadrotor unmanned aerial vehicles driven by a hybrid system of solar photovoltaic cells and energy storage batteries," Academic Journal of Science and Technology, vol. 8, no. 4, pp. 233–240, 2024.

[6] D. C. Montgomery, *Design and Analysis of Experiments*, 9th ed. Hoboken, NJ, USA: Wiley, 2017.

[7] J. A. Rosero, J. A. Ortega, E. Aldabas, and L. Romeral, "Moving towards a more electric aircraft," *IEEE Aerospace and Electronic Systems Magazine*, vol. 22, no. 3, pp. 3–9, Mar. 2007, doi: 10.1109/MAES.2007.340500.

[8] D. Scheiman, R. Walters, and S. B. Carey, "Enhanced endurance of unmanned aerial vehicles using high-efficiency Si and III-V solar cells," in Proc. 2017 IEEE Photovoltaic Specialists Conf. (PVSC), Washington, DC, USA, 2017, pp. 3842–3847.

[9] Bhutta, "Aerodynamic optimization and stability analysis of solar-powered unmanned aerial vehicle," Applied Sciences, vol. 13, no. 5, pp. 1120–1129, 2023.

[10] J. Engana Carmo and R. Lameirinhas, "Effect of photovoltaic solar panels on UAV flight endurance," Energies, vol. 14, no. 12, pp. 1533–1545, 2021.

[11] M. Saleem, S. Kumar, and R. Ramesh, "Fabrication of solar energy UAV for endurance improvement," International Journal of Ambient Energy, vol. 45, no. 3, pp. 210–218, 2020.

[12] S. Morton, N. Papanikolopoulos, and R. Siegwart, "Robotic technologies for solar-powered UAVs: Fully autonomous updraft-aware aerial sensing for multiday search-and-rescue missions," Journal of Field Robotics, vol. 34, no. 7, pp. 1235–1252, 2018.

[13] J. Kampoon, P. Maneekul, and J. Klongtrujrok, "Aerodynamics, stability, and control analysis of tactical solar-powered UAV," IOP Conf. Series: Materials Science and Engineering, vol. 106, pp. 325–330, 2020.

[14] H. M. Gonzalez Vidales, "Design, construction, and test of the propulsion system of a solar UAV," Aerospace Science and Technology, vol. 45, pp. 1–9, 2016.

[15] X. Zhan and Y. Ren, "Flight endurance extension of medium-altitude long-endurance UAV based on solar energy systems," in Proc. China Automation Congress (CAC), Beijing, China, 2022, pp. 415–420.

[16] M. S. Selig and J. F. Donovan, Airfoils at Low Speeds. H.A. Stokely, 1989, p. 45.

[17] R. Eppler, Airfoil Design and Data. Springer-Verlag, 1990, p. 112.

[18] I. H. Abbott and A. E. Von Doenhoff, Theory of Wing Sections: Including a Summary of Airfoil Data. Dover Publications, 1959, p. 78.
[19] Roskam, J. (1985). *Airplane design part I: Preliminary sizing of airplanes* (pp. 210–215). DAR Corporation.

[20] Sadraey, M. (2013). *Aircraft design: A systems engineering approach* (pp. 345–350). Wiley.

[21] Anderson, J. D. (2016). *Fundamentals of aerodynamics* (6th ed., pp. 350–400). McGraw-Hill.

[22] Raymer, D. P. (2018). *Aircraft design: A conceptual approach* (6th ed.). American Institute of Aeronautics and Astronautics (AIAA).

[23] National Renewable Energy Laboratory (NREL). (2023). *Best research-cell efficiency chart*. Retrieved from https://www.nrel.gov/pv/assets/images/cell-pv-eff-thinfilm.jpg